Heliyon 6 (2020) e04450

Contents lists available at ScienceDirect

Heliyon

journal homepage: www.cell.com/heliyon

Research article

Parametric sensitivity analysis for a natural gas fueled high temperature tubular solid oxide fuel cell

Pankaj Kalra [a,*], Rajeev Kumar Garg [a], Ajay Kumar [b]

[a] Department of Chemical Engineering, SBSSTC, Ferozepur, 152004, Punjab, India
[b] Department of Applied Science & Humanities, SBSSTC, Ferozepur, 152004, Punjab India

ARTICLE INFO

Keywords:
Chemical engineering
Chemistry
Environmental science
Solid oxide fuel cell (SOFC)
Parametric sensitivity
Triple phase boundary (TPB)
Open circuit voltage (OCV)
Power density
Current density

ABSTRACT

For more than the last two decades, there has been research going on to develop advanced energy technologies involving minimum environmental pollution, to replace the conventional fossil energy systems. Solid oxide fuel cells (SOFCs) are one of the most promising, eco-friendly and efficient means for the generation of electricity to meet the future energy requirements. This research work focuses on the parametric sensitivity analysis for natural gas fueled high temperature tubular SOFC. Firstly, for the tubular SOFC, a one-dimensional radially symmetrical model has been developed and solved using the finite-difference method. Then, the effect of the variation of important operational and design parameters on its performance has been analyzed. The parameters typically include composition, inlet fuel temperature, pressure, length of SOFC tube and thicknesses of its components. The composition is expressed as steam to methane ratio and it has been observed that the voltage and power density developed by the SOFC diminishes as the ratio increases. Further, a change in the inlet fuel pressure of the tubular SOFC has no pronounced influence on the voltage and power density developed. On the other hand, with an increase in the inlet fuel temperature, a small improvement in these performance characteristics is exhibited. The axial length of the tubular SOFC does conspicuously influence its performance characteristics but solely at current densities greater than 4000A/m^2. An increase in the thickness of its components results in a reduction in its voltage and power density developed. The largest decline in these performance characteristics with the increase in thickness is observed for electrolyte followed by cathode and anode respectively.

1. Introduction

With an increase in per-capita energy consumption globally, particularly for developed countries, there is an urgent need for the utilization of advanced and efficient green energy systems. Fuel cells have recently been investigated as an emerging technology for clean and efficient production of energy developing high conversion efficiency (typically more than 60%) and causing lower environmental pollution than conventional energy conversion systems (Larminie and Dicks, 2003). These devices convert the chemical energy stored in a fuel into electrical energy electrochemically, without the direct combustion reaction for the generation of energy from fossil fuels. Moreover, unlike conventional power generation systems, fuel cells are noiseless and maintenance-free power generation devices as they have no moving parts. So they can easily be installed in and around residential areas. Fuel cells have been demonstrated to be technologically feasible for automobiles, modular and centralized power sources (Singhal, 2002). Solid oxide fuel cells (SOFCs) are a type of fuel cells which operate at high temperatures ranging from 800 °C to 1000 °C and possess all of its components in the solid-state; even the electrolyte employed is a solid ceramic, such as Yttria stabilized Zirconia (YSZ) (Singhal and Kendall, 2003; Brus et al., 2020). These cells have recently been used for providing auxiliary power to vehicles and the generation of electricity and heat for industry. They are 50–60% efficient when employed for the generation of electricity alone, but for applications involving combined heat and power (CHP), the overall efficiency may reach 80–85% (Kalra et al., 2013; Eguchi et al., 2007). The high operating temperature supports the use of non-precious metal catalysts and promotes internal reforming of a wide variety of fuels, dispensing the cost associated with an external reformer in the system.

As the development and trial examinations of novel inventions of the SOFC system are tedious and rather a costly affair, numerical modeling and simulation of SOFCs have become a valuable tool to comprehend and provide broad insight into the processes occurring in these systems. Calise et al. (2007) have reported modeling and simulation of a 1-D

* Corresponding author.
E-mail address: pankajkalra75@gmail.com (P. Kalra).

https://doi.org/10.1016/j.heliyon.2020.e04450
Received 18 December 2019; Received in revised form 6 March 2020; Accepted 10 July 2020

tubular SOFC based on Finite Element Method (FEM), taking into consideration the detailed kinetics of reforming reactions and the water gas shift reaction in the pre-reformer,. Hao (2007) carried out 2-D modelling and simulation studies for a single chamber SOFC for varied geometries, operating conditions and fueled with different hydrocarbon fuels. Ho (2009) developed a 3D model utilizing Star-CD with its developed subroutines on a single fuel stream consisting of methane and steam fed into an anode supported SOFC. A 3-D IT planar SOFC on a similar feed has been modeled and simulated by Yuan (2010) combining the transport diffusive phenomena, thermo-physical variation and chemical source terms. Anderson (2010) applied CFD approach for modeling and simulation of IT-SOFC based upon different renewable fuels. Takino et al. (2019) modeled and simulated 3-D planar SOFC to visualize the distribution of concentration and temperature in hydrocarbon fed electrolyte supported SOFC. In the study, the exchange current density equation applicable for humidified hydrogen fuels has been modified for application to SOFCs fueled by hydrocarbons. Wu et al. (2019) conducted a parametric sensitivity analysis of important microstructural parameters of the composite anode/cathode function layers for a planar SOFC fuelled with humidified H_2 feed. Radaideh and Radaideh (2020) employed a novel approach incorporating a framework of sensitivity analysis (SA) and uncertainty quantification (UQ) methods for analysing and refining SOFC models based upon maximum power and efficiency attained.

Most of the modeling and simulation investigations of SOFCs for numerical implementation on its developed models rely on steady-state conditions, incorporating variations mainly in two and three spatial dimensions of the geometry. Also, one-dimensional modeling performed in some studies is based on the Finite Element Method (FEM) for its numerical implementation. Most of these studies have considered fuel compositions based on pure hydrogen and steam or pre-reformed product stream from reforming of hydrocarbons like methane, ethane etc. Further, barely a few studies have been reported that investigate the parametric sensitivity of a SOFC system to operational and design parameters.

During commercial utilization of SOFCs, operational disturbances (load disturbances) result in disturbing the smooth functioning of the system and hence may have a detrimental effect on its performance characteristics leading to operational difficulties. Further, the design parameters comprising of the dimensions of a SOFC system determines its economics to a large extent. The objective of this research work is a detailed investigation affecting the performance of natural gas fueled tubular SOFC due to the variation of typical operating parameters like fuel composition, temperature, pressure and design parameters involving axial length and thickness of its components. The 1-D model developed in the study fully incorporates the variation of all the properties typically density, viscosity, thermal conductivity in the gaseous system, due to a change in concentration, temperature and pressure. Moreover, high temperature in-situ reforming, water gas shift reactions along with electrochemical cell reaction kinetics have been included in the developed model. The inlet fuel composition governs the relative rates of reforming and water gas shift reactions in the anodic chamber (Mozdzierz et al., 2019). These reactions build up a concentration of H_2 (fuel) which upon further reaction with oxide ions generates an electric current. The operating pressure determines the power requirement for pumping fuel through the SOFC tube. Reaction kinetics is also significantly affected by a change in fuel pressure. The temperature of the inlet fuel stream governs the heat duty required, degradation rate and the choice of materials. The length of SOFC tube should be sufficient to provide reasonable residence time for the reforming and electrochemical cell reactions. The thicknesses of the components of a SOFC should be adequate to withstand the operating conditions and contributes to its material and manufacturing cost. In this study, the result of the variation of parameters on the performance of the tubular SOFC has been examined with respect to its Voltage and Power density developed.

2. Methodology

A steady-state simplified radially symmetrical one-dimensional model of the tubular SOFC has been developed, based upon the reaction kinetics, transport and energy equations and electrochemical behaviour.

2.1. Reaction kinetics

In a natural gas fuelled SOFC, the gas entering the flow-channel predominantly contains CH_4, H_2, CO, H_2O and CO_2 (Hao, 2007, 2008). The high operating temperature employed promotes endothermic partial and complete methane reforming reactions (PMR and CMR) and water gas shift (WGS) reactions in the fuel channel leading to the production of H_2 (fuel) (Anderson, 2010; Gallucci et al., 2004; Giuseppe et al., 2018).

$$CH_4(g) + H_2O(g) \rightleftarrows 3H_2(g) + CO(g) \quad (1)$$

$$CH_4(g) + 2H_2O(g) \rightleftarrows 4H_2(g) + CO_2(g) \quad (2)$$

$$CO(g) + H_2O(g) \rightleftarrows CO_2(g) + H_2(g) \quad (3)$$

The detailed reaction kinetics has been illustrated in previous papers (Kalra et al., 2018).

In the external circuit, the electrons migrating from the anode to the cathode react with oxygen reducing it to O^{2-} ions (Yuan, 2010).

$$½\ O_2(g) + 2e^- \rightarrow O^{2-} \quad (4)$$

A triple phase boundary (TPB) is established due to the co-existence of the electrolyte (acting as a conductor for oxide ions), porous anodic surface (solid catalyst) and the gas interface (transportation of H_2 fuel) (Liu et al., 2019).

The O^{2-} ions, generated at the cathode, travel through the permeable electrolyte to the anode where they combine with hydrogen (fuel) at the TPB generating water and e^- as per electrochemical cell reaction (ECR) (Fahs and Ghassemi, 2019).

$$H_2 + O^{2-} \rightarrow H_2O + 2e^- \quad (5)$$

2.2. Assumptions

(i) The Tubular SOFC is operating under steady-state. (ii) The fuel and air are treated to be ideal gas mixtures. (iii) The electrodes are considered to be isotropic and homogeneous. (iv) Negligible ohmic drop in an electronically conductive solid matrix of porous electrodes as well as the current collectors. (v) No radial and angular variation of velocity, concentration, temperature and current density. (vi) The SOFC is considered to be insulated at the outer wall.

2.3. Transport equations

From the perspective of transport, a single SOFC consists of several components: the flow channels (fuel channel and air channel), the electrodes (anode and cathode) and the electrolyte. The fuel and air are fed to their respective flow channels.

2.3.1. Anodic chamber

The 1-D total continuity equation for the anodic chamber is expressed as:

$$\frac{d(\rho u)}{dx} = -\frac{dP}{dx} \quad (6)$$

where ρ, u and P represent the density, velocity and pressure of the gas in the anodic chamber.

Similarly, the component continuity equation for the i^{th} component is expressed as:

$$\frac{d(uC_i)}{dx} = \left(\frac{1}{V_{anode}}\right)\sum r_i \quad (7)$$

where V_{anode} represent the volume of the anodic chamber, C_i and Σr_i- the molar concentration and the sum of rate of reaction of species i in anodic chamber.

The reforming and the water gas shift reactions occur in the fuel channel. On the other hand, the electrochemical cell reaction occurs at the TPB. The overall energy balance of the tubular SOFC system thus becomes (Calise et al, 2007, 2008):

$$\frac{d\left(u_{fuel}\rho_{fuel}Cp_{fuel}T_{fuel}\right)}{dx} + (\Delta H)_{PMR} + (\Delta H)_{CMR} + (\Delta H)_{WGS} + (\Delta H)_{ECR} = -Q_{transfered} \quad (8)$$

where u_{fuel}, ρ_{fuel}, T_{fuel} and C_{Pfuel} represent the velocity, density, temperature and specific heat of the fuel, ΔH_{rxn} - the heat associated with different reactions and $Q_{transferred}$ - the heat being transferred from the anodic to the cathodic chamber.

The detailed transport equations have been illustrated in the previous papers (Kalra et al., 2017).

2.3.2. Cathodic chamber

The 1-D conservation equation for the cathodic chamber is expressed as:

$$\frac{d(uC_{O_2})}{dx} = \left(\frac{1}{V_{cathode}}\right)r_{O_2} \quad (9)$$

where $V_{cathode}$ represent the volume of the cathodic chamber, C_{O2} and r_{O2} - the molar concentration and the rate of reaction of oxygen.

The rate of change in concentration of oxygen is predicted by Faraday's law:

$$r_{O_2\ reacted} = -\frac{i_{H_2}}{4F} \quad (10)$$

where i_{H2} represents the current generation due to H_2 oxidation and F -the Faraday's constant.

The energy balance for the air channel is governed by the heat flow from anode to cathode:

$$\frac{d(u_{air}\ \rho_{air}Cp_{air}\ T_{air})}{dx} = Q_{transferred} \quad (11)$$

where u_{air}, ρ_{air}, T_{air} and C_{Pair} represent the velocity, density, temperature and specific heat of the air in the cathodic chamber.

2.4. Electrochemical behaviour

The ideal electrical potential developed ($E_{ideal,\ H2}$) due to the electrochemical cell reaction is predicted by the Nernst equation (Mobarak and Alshehri, 2020):

$$E_{ideal,H_2} = \frac{1}{2F}\left[\Delta G_{H2\ oxid.}(T) + RT\ln\frac{P_{H_2}P_{O_2}^{\frac{1}{2}}}{P_{H2O}}\right] \quad (12)$$

where $\Delta G_{H2\ oxid}$ represents Gibb's free energy change associated with the H_2 oxidation reaction, P_{H2}, P_{O2}, P_{H2O} - represent the partial pressures of hydrogen, oxygen and steam respectively.

The Nernst equation ideally predicts an increase in open circuit voltage (OCV) with an increase in fuel pressure (Bove and Ubertini, 2008). Certain Polarization losses lead to a drop in potential developed from the Nernst Potential or OCV. These are - ohmic polarization, activation polarization and concentration polarization.

The electrical resistance of components of the SOFC leads to ohmic polarization loss η_{ohm} (Radaideh and Radaideh, 2020):

$$\eta_{ohm} = i\left(\frac{t_{anode}}{\sigma_{anode}} + \frac{t_{electolyte}}{\sigma_{electrolyte}} + \frac{t_{cathode}}{\sigma_{cathode}}\right) \quad (13)$$

where i represents the current density, t_{anode}, $t_{electrolyte}$, $t_{cathode}$ - the thicknesses and σ_{anode}, $\sigma_{electrolyte}$, $\sigma_{cathode}$ - the conductivities of anode, electrolyte and cathode respectively.

The activation polarization loss $\eta_{act}$is determined by the Tafel equation (Yonekuraa et al., 2011):

$$\eta_{Act} = \frac{RT}{nF}\left\{\frac{i}{io}\right\} \quad (14)$$

where n-no. of electrons transferring during cell reaction.

The total exchange current density i_0 in the Tafel equation has been ascertained using Butler-Volmer equation from respective exchange current densities of cathode i_{Oc} and anode i_{Oa} (Mahcene et al., 2011, Takino et al. 2019):

$$i_{OC} = \gamma_C\left(\frac{P_{O_2}}{P_{O_{2,ref}}}\right)^C \exp\left(\frac{-E_{act,c}}{RT_a}\right) \quad (15)$$

$$i_{Oa} = \gamma_a\left(\frac{P_{H_2}}{P_{H_{2,ref}}}\right)^A\left(\frac{P_{H_2O}}{P_{H_2O,ref}}\right)^B \exp\left(\frac{-E_{act,a}}{RT_a}\right) \quad (16)$$

$$i_O = \left(\frac{1}{i_{O_C}} + \frac{1}{i_{O_a}}\right) \quad (17)$$

where P_{H2ref}, P_{O2ref}, P_{H2Oref} - represent the reference partial pressures of hydrogen, oxygen and steam respectively, $E_{act,a}$ -the activation energy and A, B, C are constants.

The concentration polarization losses η_{conc} for the respective anodic and cathodic regions have been determined using the relations (Pasaogullari and Wang, 2003; Yonekuraa et al., 2011):

$$(\eta_{Conc})_{anode} = \frac{RT}{nF}\ln\left(1 - \frac{i}{ias}\right) \quad (18)$$

$$(\eta_{Conc})_{cathode} = \frac{RT}{nF}\ln\left(1 + \frac{P_{H2}}{P_{H2O} \times i_{as}}\right) + \frac{RT}{nF}\ln\left(1 - \frac{i}{i_{cs}}\right) \quad (19)$$

The limiting current densities i_{as} and i_{cs} employed in these relations has been computed as:

$$i_{as} = \frac{2F\ P_{H2}^a D_{a\ eff}}{R\ T\ l_a} \quad (20)$$

$$i_{cs} = \frac{4F\ P_{O2}^c D_{c\ eff}}{\left(\frac{P_t - P_{O2}^c}{P_t}\right)RTl_c} \quad (21)$$

where $D_{a,eff}$, $D_{c,eff}$ represent the effective diffusivity in anodic and cathodic regions, P_t - the total pressure, l_a and l_c- the height of anodic and cathodic chambers respectively.

The algebraic summation of concentration polarization losses in the anodic and cathodic regions of the SOFC provides the means for determining the total concentration polarization loss. The net voltage developed by the Tubular SOFC thus becomes (Nafees and Abdul Rasid, 2019):

$$V_{net} = V_0 - \eta_{act} - \eta_{conc} - \eta_{ohm}$$

$$V_{net} = -\frac{\Delta G^0}{2F} - \ln\frac{P^0_{H2O}}{P^a_{H2}\times P^c_{O2}} - i\left(\frac{l_{anode}}{\sigma_{anode}} + \frac{l_{electolyte}}{\sigma_{electrolyte}} + \frac{l_{cathode}}{\sigma_{cathode}}\right) - \frac{RT}{nF}\ln\left(1-\frac{i}{ias}\right) - \frac{RT}{nF}\ln\left(1+\frac{P_{H2}}{P_{H2O}\times i_{as}}\right) + \frac{RT}{nF}\ln\left(1-\frac{i}{i_{cs}}\right) - \frac{RT}{nF}\left(\frac{i}{io}\right) \quad (22)$$

2.5. Boundary conditions

(i) Air channel

•At $r = r_{cathode\ surface}$, the cylindrical wall of the air channel, i.e. $0 \le x \le L$, L being the total length of SOFC tube.

$$T_{air} = T_{cath.\ surface}$$
$$h\left(T_{cath.\ surf} - T_{air}\right) = Q_{cathode\ surface} \quad (23)$$

where T_{air}, $T_{cath.\ surface}$ - represent the temperatures of air channel and cathodic surface, $Q_{cathode\ surface}$ -the heat associated with the cathodic surface.

•At the inlet to the air channel, i.e. $x = 0$

$u = u_{i,air}$, $C = C_{Pair}$, $T = T_{a,i}$

(ii) Fuel channel

•At $r = r_{in}$, the inner cylindrical wall of the fuel channel, $0 \le x \le L$

$$T_{fuel} = T_{anode\ surface}$$
$$h\left(T_{fuel} - T_{anode\ surface}\right) = Q_{cathode\ sueface} = Q_{anode\ surface} \quad (24)$$

where $T_{anode\ surface}$ - represent the temperature of anodic surface. $Q_{anodesurface}$ -the heat associated with the anodic surface.

•At the inlet to the fuel channel, i.e. $x = 0$

$u = u_{i,fuel}$, $C = C_{i,fuel}$, $T = T_{fi}$

2.6. Discretization and numerical implementation

A finite-difference based discretization of the steady one-dimensional radially symmetric model has been implemented and variation of physical properties along the axial direction has been incorporated exploiting standard correlations for these properties (Yaws, 2015).

The SOFC tube has been discretized along its axis by means of planes orthogonal to the axis of the cylindrical tube, developing 100 axial nodes. The computational procedure for the solution of model equations consisting of mass, energy and momentum balance for anodic and cathodic chambers has been implemented through in-house codes developed in Matlab platform. The model developed has been validated against Siemens Westinghouse tubular SOFC experimental data and the results have been illustrated in the previous papers (Kalra et al., 2017) (See Figure 1).

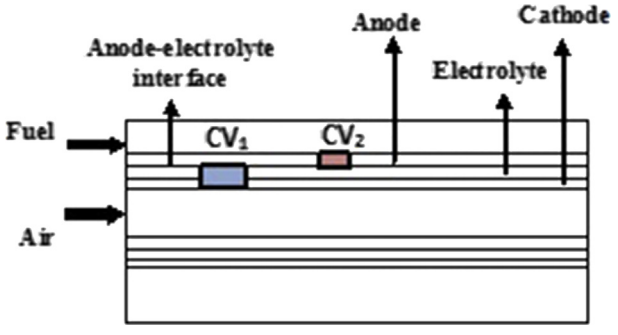

Figure 1. One dimensional discretization of Tubular SOFC.

3. Results and interpretation

In this research work, the parametric sensitivity analysis has been investigated for a 1-D radially symmetric natural gas fueled tubular SOFC. The composition of the feed stream and the conditions of operation has been stated in previous papers (Kalra et al., 2017). The simulated results have been compiled in terms of the characteristic V–I and PD-I plots.

3.1. Effect of variation of fuel composition

For studying the effect of variation of fuel composition, the composition of the fuel stream has been varied by changing the partial pressure of the key reactants (i.e. steam and methane), responsible for the production of H_2 (fuel). The partial pressure of other components in the fuel stream is kept constant. The resulting concentrations expressed as the molar ratio of steam to methane are tabulated in Table 1.

For the tabulated range of concentrations ratios so obtained, the performance characteristics curves of V–I and PD-I have been depicted in Figures 2(a) and 2(b).

Figure 2 (a) depicts that for a specific value of current density the developed voltage drops as molar steam/methane ratio increases. It is observed that for a typical current density of 1000 A/m^2, the developed voltage drops from 0.7V to 0.6V as steam/methane ratio increases from 1.35 to 6.09. An increase in mole fraction of steam/methane ratio results in a decreased concentration of methane relative to steam available for reforming reactions. The decreased rate of the reactions results in hydrogen starvation conditions. The decreased concentration of H_2 available at TPBs limits the rate of electrochemical cell reaction resulting in a decrease in the developed voltage, thereby adversely affecting the performance of the SOFC. At the higher current densities, the developed voltage diminishes to a lesser extent for a comparable increase in steam/methane ratios. This decrease in the difference of the developed voltage with increasing steam/methane ratio at higher current densities is attributed to the fact that the cell reaction occurs at a high rate for all the cases of the fuel composition. Oprych et al. (2007) reported CFD modelling and simulation of a 3-D planar SOFC fueled with a mixture of H_2 and N_2 employing commercial ANSYS 15.0 Fuel Cell Tools module. The CFD analysis aimed at determining a desirable mass flow rate of hydrogen to be fed to the SOFC in order to prevent fuel starvation. The study reveals that on the operation of the SOFC at two different mass flow rates of 4.9×10^{-8} and 9.9×10^{-8} kg/s, a decrease in cell voltage ranging from 20% to 30% under hydrogen starvation conditions is observed resulting in significant declivities in the electric current. An increase in steam/methane ratio as deliberated in our study results in

Table 1. Voltage and Power density for molar ratios $Y_{steam}/Y_{methane}$.

$Y_{steam}/Y_{methane}$	1.35	2.02	2.70	3.38	4.05	4.75	5.41	6.09
Voltage	V_1	V_2	V_3	V_4	V_5	V_6	V_7	V_8
Power density	PD_1	PD_2	PD_3	PD_4	PD_5	PD_6	PD_7	PD_8

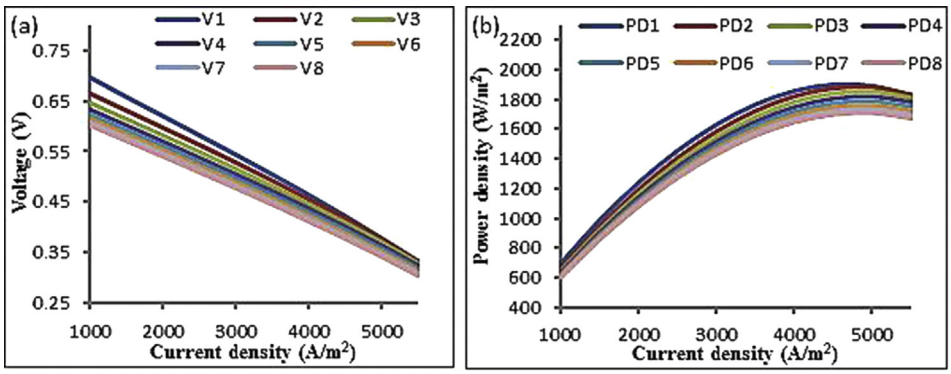

Figure 2. Effect of variation of composition on the (a) Voltage and (b) Power density.

hydrogen starvation conditions and an analogous concordant descent in its performance characteristics.

Similarly, the effect of variation of steam/methane ratio on the PD-I characteristic curves as depicted in Figure 2(b), predicts that for a specific value of current density, an increase in the steam/methane ratio results in a reduction in the developed power density. The reduction in power density with increasing steam/methane ratio has been observed to be maximum for current density ranging from 2500A/m^2 to 5000A/m^2. At lower current densities (<2500 A/m^2), due to the lesser contribution of polarization losses, a relatively smaller decrease in power density is affected, thereby neutralizing the effect of the increase in steam/methane ratio to a large extent. For current densities ranging from 2500A/m^2 to 5000A/m^2, the combined contribution of higher polarization losses and detrimental influence of steam/methane ratio, together are responsible for a substantial reduction in power density. At still higher values of current densities (>5000A/m^2), the developed voltage reduces sharply, power density is the product of V and I, the increased current density tends to diminish the effect of higher steam/methane ratio, so these curves tend to converge.

3.2. Effect of variation of total fuel pressure

The effect of variation of the total fuel pressure on the performance characteristics of the tubular SOFC for pressures ranging from 1bar to 5bar (in increments of 1bar) in terms of V–I and PD-I bar charts, has been depicted in Figure 3.

A set of clustered bars in these figures represent the comparative voltage and power density developed for a specific value of current

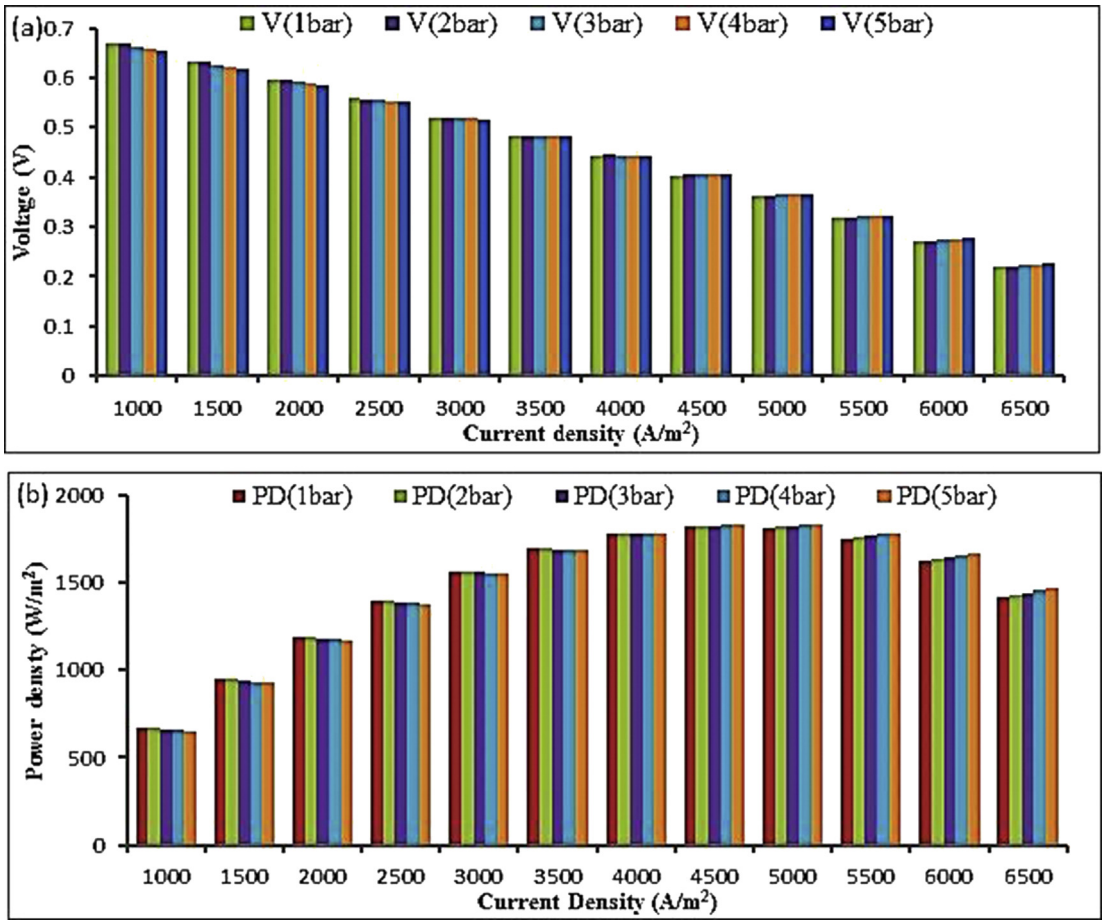

Figure 3. Effect of variation of total fuel pressure on the (a) Voltage (b) Power density.

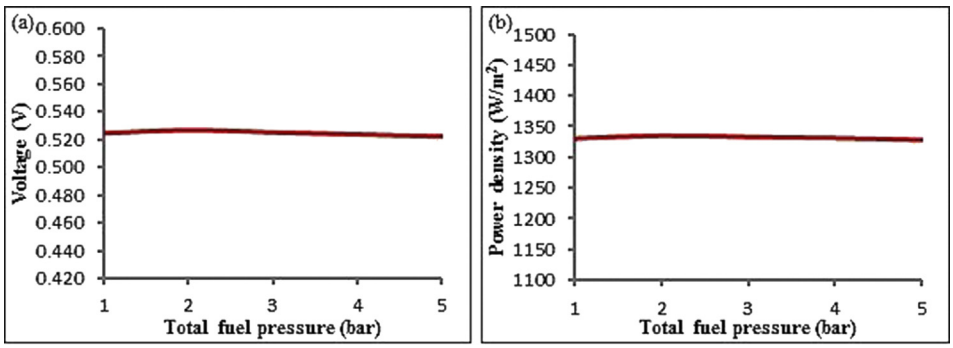

Figure 4. Effect of variation of fuel pressure on (a) Avg. Voltage (b) Avg. Power density.

density, for the range of the fuel pressures. The comparably identical heights of these clustered bars representing the V–I and PD-I data for the range of fuel pressures suggest no significant influence of variation of fuel pressure on the voltage and power density developed. Further, a slight improvement in the performance characteristics has been observed, with an increase in fuel pressure, particularly for current densities >4000 A/m^2. However, this improvement can be ignored for all practical purposes. Thus the study predicts that the performance of the tubular SOFC is essentially independent of the total fuel pressure for the feasible and economic range of pressures being analyzed.

The pressure dependence of the performance characteristics of the tubular SOFC has been supplemented with the determination of average voltage and power density for the range of current density being employed (1000A/m^2 - 6500A/m^2), and plotting against the total fuel pressure as illustrated in Figure 4.

The figures reveal a small influence of the total fuel pressure on the average voltage and power density developed. The average voltage increases infinitesimally from 0.525V to 0.527V and subsequently the power density developed from 1330W/m^2 to 1336W/m^2 as the fuel pressure rises from 1bar to 2bar. The small improvement in the performance characteristics at low pressure range may be attributed to the increase in Nernst potential. An increase in the fuel pressure above 2bar is accompanied with a slight decrease in voltage and power density developed. For higher pressures, voltage drop resulting from concentration polarization overcomes the positive contribution due to increase in Nernst potential. Thus, at higher operating fuel pressure range, the cumulative effect of escalation in Nernst Potential and concentration

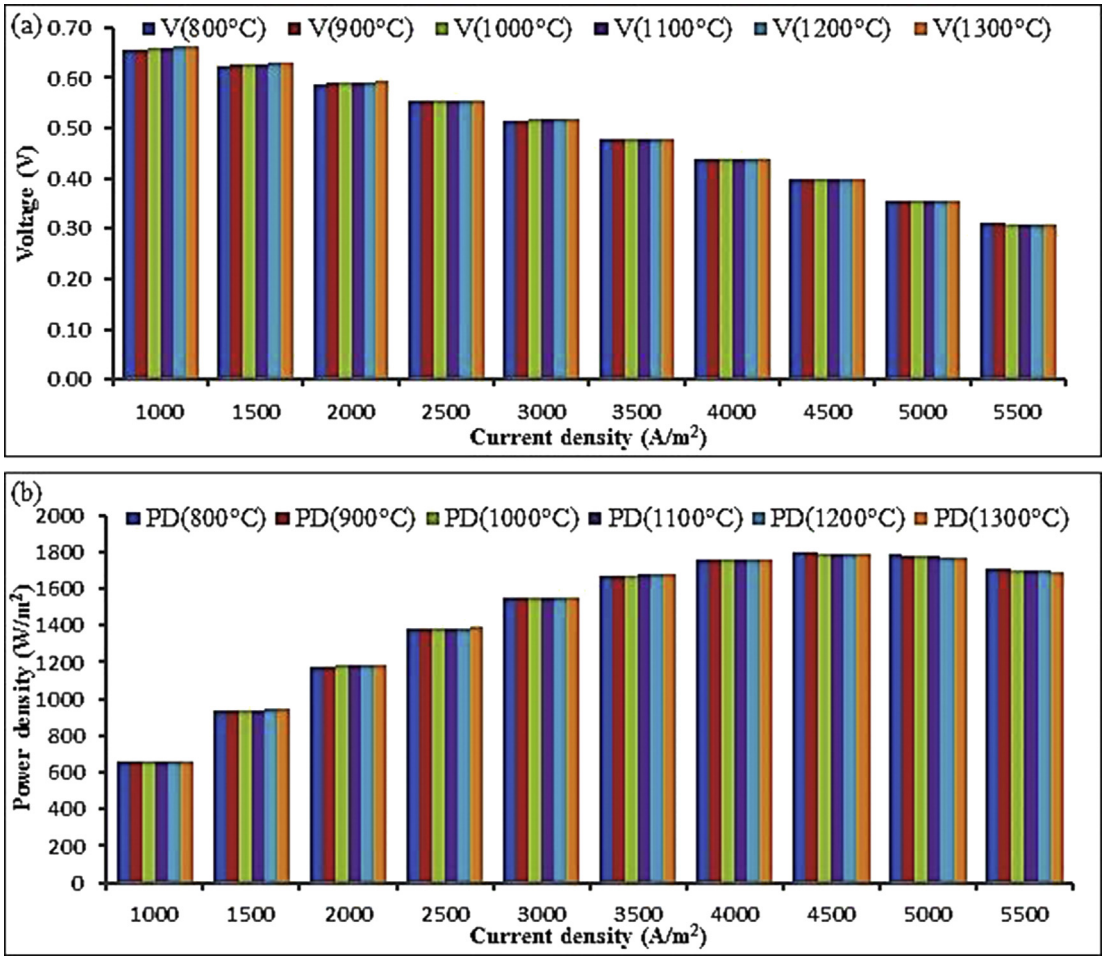

Figure 5. Effect of variation of fuel temperature on the (a) Voltage (b) Power density.

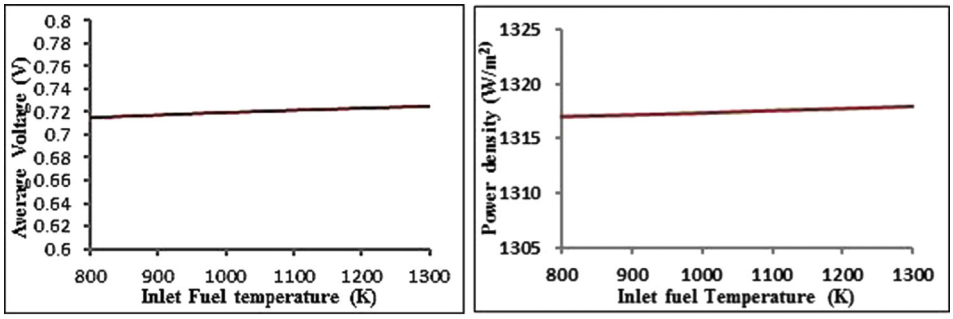

Figure 6. Effect of variation of fuel temperature on (a) Avg. Voltage (b) Avg. Power density.

polarization results in a net decline in average voltage and power density and its performance characteristics.

3.3. Effect of variation of inlet fuel temperature

In this section of the study, the response of the performance characteristics of the tubular SOFC to an alteration in the inlet fuel temperature has been analyzed in the range 800K–1300K in increments of 100K. The inlet fuel temperature for a SOFC governs the rates of endothermic reforming and water gas shift reactions, which are largely responsible for the generation of H_2(fuel). The result of the change in the inlet fuel temperature on the V–I and PD-I performance characteristics have been represented in the form of clustered bar charts depicted in Figures 5(a) and 5(b).

The clustered bar charts, portraying different temperatures for a specific current density, clearly show only a meagre effect on the voltage and power density developed with a change in inlet fuel temperature. A close analysis of these bar charts shows that at lower current densities, an increase in inlet temperature results in a small increase in voltage and power density which reverses its trend at higher current densities.

There is a linear dependence of concentration and activation polarization losses with temperature. Conversely, the ohmic polarization losses decrease with an increase in temperature. The small increase in voltage and power density observed at lower current densities is attributed to a reduction in ohmic polarization losses. At higher current densities, an increase in concentration and activation polarization losses overshadows the decrease in ohmic resistance resulting in a net decrease in voltage and power density.

The temperature dependence study of the performance characteristics of the tubular SOFC has been further supplemented with the determination of average voltage and power density for the range of current density (1000A/m^2 to 5500A/m^2). The results are illustrated in Figure 6.

Figure 6(a) portraying the effect of variation of fuel temperature on the average voltage developed by the tubular SOFC exhibits a small linear increase in average voltage from 0.715V to 0.725V with an increase in temperature from 800 to 1300K. An analogous behaviour on the average power density developed as illustrated in Figure 6(b) is observed with the increase in fuel temperature. A net small increase of 2 W/m^2 in the power density developed has been observed with the corresponding increase in fuel temperature. This small linear increase in average voltage and power density with a rise in temperature may be attributed to a net decrease in polarization losses at higher temperatures. Wu et al. (2019) developed a quasi–2-D non-isothermal microstructural based model of a SOFC for its parametric simulation and optimization. In the study, the effect on the voltage developed associated with a variation of microstructural parameters for three different temperatures 1023/1073/1123K has been investigated. For a decrease in temperature from 1123K to 1023K, the study predicts a curvilinear drop in voltage ranging from 0.025V at 1000 A/m^2 to as high as 0.25V at 7000 A/m^2. The trends of results illustrated in this study are similar to that being observed for the variation of temperature as depicted in the present investigation.

3.4. Effect of variation of length

In this section of the study, the axial length of the tube of the tubular SOFC is varied between the 0.6m and 2.0m in increments of 0.2m. The result of this variation on its performance characteristics is represented in terms of V–I and PD-I curves and depicted in Figure 7.

The overlapping curves depicted in Figure 7(a) for current densities <4500 A/m^2, clearly show no significant influence on voltage developed as the length of SOFC tube increases. On the other hand, a curvilinear drop in voltage has been observed for larger current densities (>4500 A/m^2), as the SOFC tube lengthens.

An analogous behaviour has been noticed in PD-I performance curves depicted in Figure 7(b). The PD-I performance curves for different

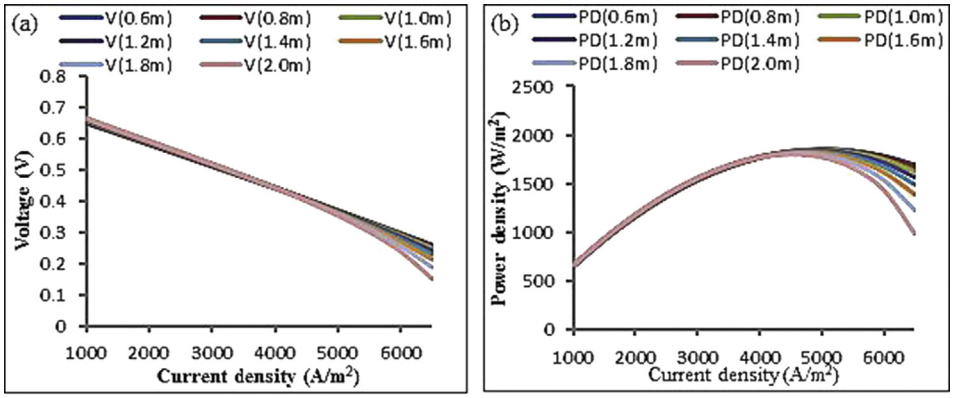

Figure 7. Effect of variation of length of SOFC on (a) Voltage (b) Power density.

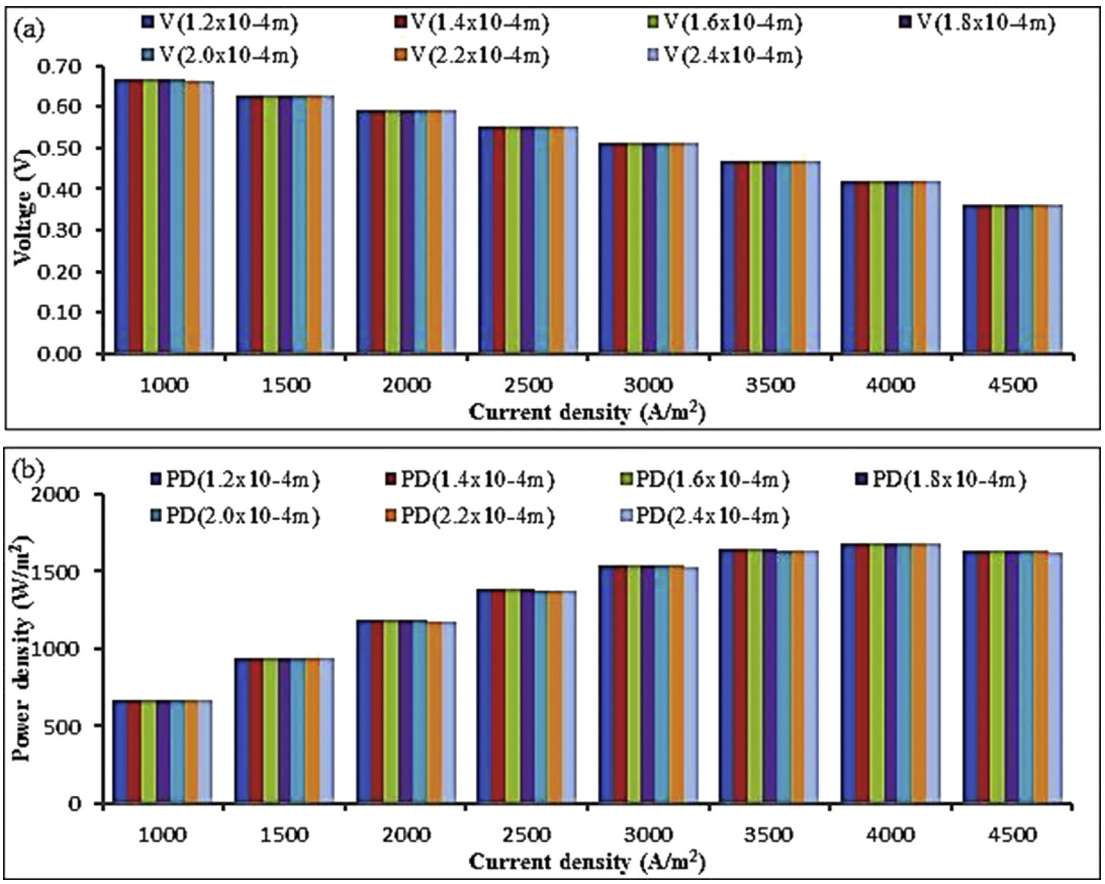

Figure 8. Effect of variation of thickness of anode on (a) Voltage (b) Power density.

lengths of SOFC tube overlap each other for current densities <4500A/m^2, showing the insensitivity of the power density distribution to the increase in its length. The usual drop in power density from maxima at higher current densities has been observed for current densities >4500 A/m^2, exhibiting a more curvilinear path as SOFC tube lengthens. This sharp decrease in its performance characteristics at higher current densities, as the SOFC tube lengthens, is attributed to the larger contribution of the concentration polarization losses. Thus, smaller length SOFCs develops larger voltage and power density per unit length due to lower polarization losses. However, for a given service, the number of small length SOFCs required may become very large. For the typical fixed parameters values investigated in this study, the results predict that for length of SOFC tube >1.4m, the drop in voltage and power density developed becomes substantial.

3.5. Effect of variation of thicknesses of components

In this section of parametric sensitivity, the performance analysis to a variation in thickness of the functional design components– cathode, anode and electrolyte of the tubular SOFC has been investigated by varying them individually keeping the thickness of other components and other parameters constant.

3.5.1. Anode

In the investigation, the result of a change in thickness of the anode has been analyzed by its variation between 1.2×10^{-4} and 2.2×10^{-4}m in increments of 0.2×10^{-4}m. The effect of this variance on its performance characteristics has been examined in terms of the V–I and PD-I clustered bar graphs depicted in Figure 8.

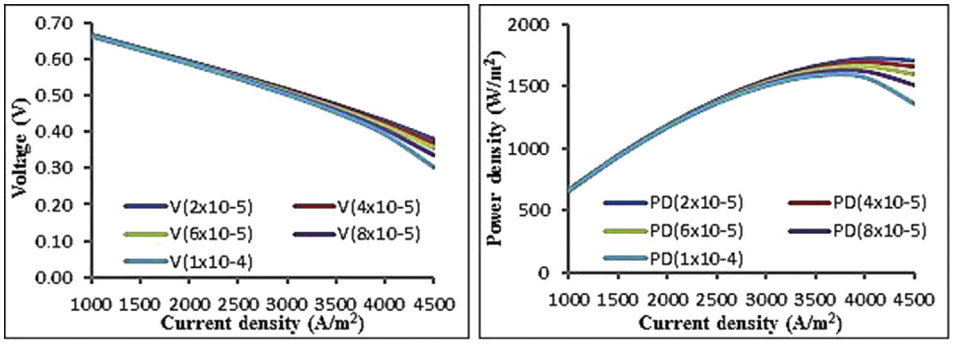

(a) **(b)**

Figure 9. Effect of variation of thickness of cathode on (a) Voltage (b) Power density.

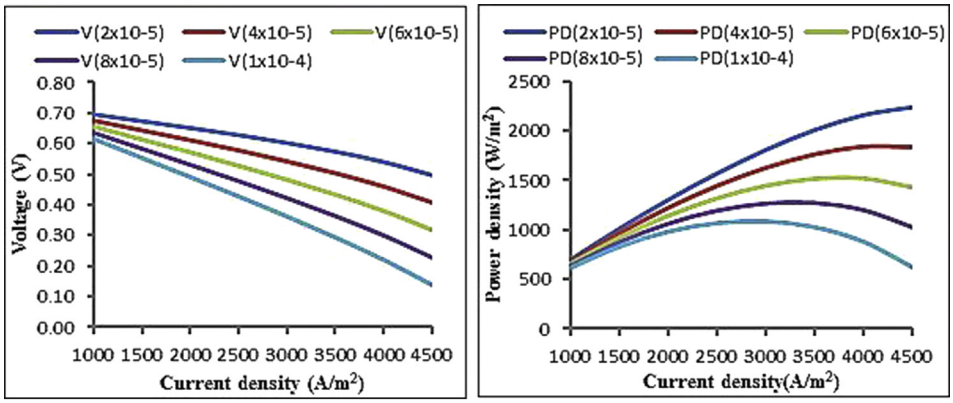

Figure 10. Effect of variation of thickness of electrolyte on (a) Voltage (b) Power density.

As shown in the figure, for a particular current density, the comparable height of clustered bars for different thicknesses of anode of the tubular SOFC illustrate no significant influence of the variation in thickness of the anode on its performance characteristics.

This insensitivity of the performance of the SOFC to the variation in thickness of anode is attributed to the fact that the electrical conductivity of anodic material is the highest amongst its components and hence poses minimal ohmic resistance despite the increased thickness. The high electrical conductivity and low ohmic resistance of typical commercially employed anodic materials like Ni/YSZ allow usage of thicker anodic layers for providing strength to SOFCs. Thus, anodes can be commercially employed as the most probable substrate component for supporting other components of SOFC without any detrimental effect on its performance.

3.5.2. Cathode

In this section of the study, the thickness of the cathode of the tubular SOFC has been varied between 0.2×10^{-4} and 1.0×10^{-4}m in increments of 0.2×10^{-4}m and the result in the form of its performance characteristics has been depicted in terms of V–I and PD-I curves as depicted in Figure 9.

The overlapping V–I curves for current densities <3000 A/m^2, as depicted in Figure 9(a), clearly reveal that the thickness of cathode does not significantly influence the developed voltage at these lower current densities. Further, a sharp decline in voltage developed with an increase in cathodic thickness for higher current densities (>3000 A/m^2) has been observed. The comparably alike developed voltage for different thicknesses of cathodes at lower current densities is attributed to the negligibly small contribution of cathodic ohmic overpotentials at these lower current densities. The contrasting behaviour at high current densities is attributed to a sharp increase in ohmic over-potential due to complementary effects of higher current density and higher cathode thickness.

The PD-I performance characteristic curves depicted in Figure 9(b) show usual characteristics, a linear increase in the power density developed for current densities up to 3000 A/m^2 and then a curvilinear drop for current density typically >3500 A/m^2. The curvilinear drop in power density developed at higher current densities is observed to be sizable for thicker cathodic layers. Analogous to V–I distribution, the overlapping PD-I curves at lower current densities, clearly show the insensitivity of the power density developed to an increase in cathodic thickness. The result of this analysis clearly establishes that thicker supporting cathodes could only be employed for SOFC systems operating predominantly at lower current densities.

3.5.3. Electrolyte

In this section of the study, the thickness of electrolyte of the tubular SOFC is varied between 0.2×10^{-4}m and 1.0×10^{-3}m in increments of 0.2×10^{-4}m and the result of this variation is interpreted in form of V–I and PD-I performance characteristics curves, as depicted in Figure 10.

The segregated V–I performance characteristics curves for the different thicknesses of electrolytes of the tubular SOFC depicted in Figure 10(a) characterize a substantial drop in voltage with an increase in the thickness of the electrolytic component. Moreover, the operation of thicker electrolytic SOFCs at high current densities results in even a considerably larger drop in the developed voltage. It can be clearly visualized from the figure that for a typical current density of 3500 A/m^2, an increase in the thickness of the electrolyte from 0.2×10^{-4} to 1.0×10^{-3} m, results in a reduction in the voltage developed to half its initial value (0.6V–0.3V). This large decline in developed voltage for thicker electrolytic SOFCs is attributed to the low electron conductivities of these components; its thicker layers contributing substantially to the larger ohmic over-potential losses.

As depicted in Figure 10(b), analogous behaviour for PD-I performance characteristics has been observed for differently thickened electrolytes of the tubular SOFC. For a particular value of electrolytic thickness, the PD-I characteristic curves exhibit usual behaviour; increasing linearly with an increase in current density, reaches a maximum and then decreases. However, it has been observed that for a particular current density, thicker electrolytic SOFCs develop appreciably lower values of power densities. For the same typical current density of 3500 A/m^2, the maximum power density developed reduces to half its initial value with an increase in the thickness of the electrolyte from 0.2×10^{-4} to 1.0×10^{-3}m. Further, it has been observed that the point of maximum power density shifts to a relatively lower value of current density as the thickness of the electrolyte increases. This dynamic behaviour of the performance characteristics of the tubular SOFC is attributed to a large contribution to over-potential losses for thicker electrolytic SOFCs.

The implications of the results obtained for this variation in thicknesses of components is that the commercially employed electrolytic materials pose maximum ohmic resistance; hence, its thicker layers result in a sizeable decline in performance characteristics of the SOFC, contrary to the case for the thickness of anode and cathode, which have only small influence that too at higher current densities. The study, therefore predicts that SOFCs should employ thinnest electrolytes for developing high Voltage and power densities. Radaideh and Radaideh (2020), proposed a framework of Sensitivity analysis (SA) and uncertainty quantification (UQ) methods for efficiently analyzing design parameters and their effects. In the study, the Sensitivity analysis has been performed using (i) local SA with linear perturbations (ii) Morris screening (iii) Standardized regression coefficients (SRC) and (iv) Partial regression coefficients (PRC). The uncertainty quantification (UQ) methods employed were (a) deterministic-based UQ and (b) sampling-based UQ. The result of the

sensitivity analysis has been analyzed in terms of (a) power output and (b) system efficiency. The normalized results of the sensitivity analysis predict a negative sensitivity coefficient with increasing thickness. The performance characteristics (power output) of the study reveal that the electrolytic thickness is 100 times relatively hyper-sensitive than anode thickness and 40 times relatively hyper-sensitive than cathodic thickness. The outcomes of the study are congruent to the results obtained in our investigation. Thus, for optimum performance characteristics, a SOFC should have the thickest anodic layer (substrate) and thinnest electrolytic layer.

4. Conclusion

Operation of a SOFC generally results in complex internal temperature, species, and current density profiles, which are not taken into consideration in the simple thermodynamic model. From an engineering viewpoint, a good SOFC model relates to its ability to ascertain the available voltage and power density for a definite load profile. The main obstacle in developing an accurate SOFC dynamical model is the lack of information about the exact values of the modeling parameters to be employed. The inconsistent results obtained from measurements and calculations emanate due to uncertainties stemming not only from experimental assessment but also from ill-defined parameters. The choice of parameter values may significantly affect the voltage and power developed and thermal degradation characteristics of the simulated SOFC stack. The values of parameters employed in modeling are primarily based on the limited experimental data. To arrive at the optimum design and operation of the SOFC, a parametric sensitivity analysis is therefore of utmost importance to examine the set of parameters that can match modern SOFC performance expectations.

In this research work, parametric sensitivity, of the simulated natural gas fueled 1-D tubular SOFC, to important operating and design parameters has been examined by analyzing the results obtained from the characteristic V–I and PD-I plots. The study reveals that an increase in molar steam/CH_4 in the feed stream adversely affects its performance due to the reduced concentration of H_2 (fuel) available for the Electrochemical cell reaction. Thus, the study is helpful in determining a minimum desired concentration of CH_4 to be fed into an in-situ reformed SOFC to develop substantial voltage and power density characteristics. The result of the variation of inlet fuel pressure of the SOFC clearly exhibits no significant influence on its performance characteristics although it does influence Nernst potential and polarization losses to some extent. Nevertheless, the study predicts that an optimum fuel pressure for the reliable operation of the SOFC should lie between 1bar to 2bar. The result of variance in inlet fuel temperature of the tubular SOFC demonstrates slightly improved performance characteristics at higher operating temperatures owing to a decreased ohmic resistance. Consequently, the inlet fuel temperature should be maintained at the highest possible level taking material constraints into consideration.

The design parameters examined in this study are the length of the tubular SOFC and the thickness of its components. Although increasing the length of the SOFC tube enhances the residence time for reactions occurring in the fuel channel (reforming and water gas shift reactions), it also adversely affects its performance due to an increase in polarization losses. Therefore the study recommends optimum SOFC tube length of 1–1.5m based upon opposing factors of residence time and polarization losses. A comparative analysis of varying the thickness of the anode, cathode and electrolyte on the performance characteristics of the SOFC has also been explored. It has been concluded from the study that the performance of the SOFC is adversely affected with an increasing thickness of the electrolyte followed by the cathode and the anode, in that order. The electrolytic materials are insulators to electronic current, therefore should be the thinnest in order to minimize polarization losses. On the other hand, the anodic materials possess highest electronic conductivity, so thicker layers are permissible for providing mechanical strength and act as substrate, upon which thin layers of electrolyte and cathode may be preferentially deposited. Therefore, the anode supported SOFCs are the best candidates as compared to cathode or electrolyte supported ones for administering optimal performance characteristics.

The parametric sensitivity analysis for design and operating parameters has been performed on 1-D tubular SOFC. A more comprehensive analysis of parametric sensitivity must include variation along both axial and radial directions.

Declarations

Author contribution statement

Pankaj Kalra: Conceived and designed the experiments; Performed the experiments; Analyzed and interpreted the data; Contributed reagents, materials, analysis tools or data; Wrote the paper.

Rajeev Kumar Garg: Conceived and designed the experiments; Analyzed and interpreted the data; Contributed reagents, materials, analysis tools or data; Wrote the paper.

Ajay Kumar: Conceived and designed the experiments; Analyzed and interpreted the data; Wrote the paper.

Funding statement

This research did not receive any specific grant from funding agencies in the public, commercial, or not-for-profit sectors.

Competing interest statement

The authors declare no conflict of interest.

Additional information

No additional information is available for this paper.

References

Anderson, M., 2010. Review on modeling development for multiscale chemical reactions coupled transport phenomena in solid oxide fuel cells. Appl. Energy 87, 1461–1476.

Bove, R., Ubertini, S., 2008. Modelling Solid Oxide Fuel Cells Methods, Procedures and Techniques. Springer Science Business Media. B.V.

Brus, G., Iwai, H., Szmyd, J.S., 2020. An anisotropic microstructure evolution in a solid oxide fuel cell anode. Nanoscale Res Lett 15 (3).

Calise, F., Dentice d'Accadia, M., Palombo, A., Vanoli, L., 2007. A detailed one dimensional finite-volume simulation model of a tubular SOFC and a pre-reformer. Int. J. Therm. 10 (3), 87–96.

Calise, F., Dentice d'Accadia, M., Palombo, A., Vanoli, L., 2008. One-dimensional model of a tubular solid oxide fuel cell. J. Fuel Cell Sci. Technol. 5, 021014-1-15.

Eguchi, K., Singhal, S.C., Yokokawa, H., Mizusaki, J., 2007. Solid oxide fuel cells 10 (SOFC-X). Electrochem. Soc. Trans. 7 (1). ECS, Pennington, NJ.

Fahs, I.-E., Ghassemi, M., 2019. Sensitivity analysis of thermal stress in a cathode porous electrode for a planar solid oxide fuel cell. Energy Sources, Part A Recovery, Util. Environ. Eff. 1–14.

Gallucci, F., Paturzo, L., Basile, A., 2004. A simulation study of the steam reforming of methane in a dense tubular membrane reactor. Int. J. Hydrogen Energy 29, 611–617.

Giuseppe, L., De, Petronilla, F., 2018. Electrical and thermal analysis of an intermediate temperature IIR-SOFC system fed by biogas. Energy Sci. and Engg. 6 (2), 60–72.

Hao, Y., 2007. Numerical modeling of single-chamber SOFCs with hydrocarbon fuels. J. Electrochem. Soc. 154 (2), B207–B217.

Hao, Y., 2008. Numerical study of heterogeneous reactions in an SOFC anode with oxygen addition. J. Electrochem. Soc. 155 (7), B666–B674.

Ho, T.X., 2009. Numerical analysis of a planar anode-supported SOFC with composite Electrodes. Int. J. Hydrogen Energy 34.

Kalra, P., Garg, R., Kumar, A., 2013. Solid oxide fuel cell - a future source of power and heat generation. In: Engineering Applications of Nanoscience and Nanomaterials, Special Edition of Material Science Forum, 757. Trans Tech Publications, Switzerland, pp. 217–241.

Kalra, P., Garg, R., Kumar, A., 2017. Electrochemical analysis of an anode-supported axially symmetrical one dimensional tubular solid oxide fuel cell. Ind. J. of Sci. and Technol. 10 (19).

Kalra, P., Garg, R., Kumar, A., 2018. Kinetics analysis of reactions at triple phase boundaries of anode supported tubular solid oxide fuel cell. Asian J.of Chem. 30 (3), 561–566.

Larminie, J., Dicks, A., 2003. Fuel Cell Systems Explained. John Wiley & Sons Ltd (alk. paper) TK2931.L37 2003 621.31 2429 – dc21 2002192419.

Liu, S.-S., et al., 2019. Atomic structure observations and reaction dynamics simulations on triple phase boundaries in solid-oxide fuel cells. Communications Chemistry 2, 48.
Mahcene, H., Moussa, H.B., Bouguettaia, H., Bechki, D., Zeroual, M., 2011. Computational modeling of the transport and electrochemical phenomena in solid oxide fuel cells. Energy Procedia 6 (2011), 65–74.
Mobarak, Y.A., Alshehri, A.A., 2020. PI and hysteresis current controller for grid-connected dynamic state configuration model of solid oxide fuel cell SOFC. Int. J. Recent Technol. Eng. 8 (5), 1975–1980.
Mozdzierz, M., et al., 2019. A multiscale Approach to the numerical simulation of the solid oxide fuel cell. Catalysts 9 (253), 1–28.
Nafees, A., Abdul Rasid, R., 2019. Study of natural gas powered solid oxide fuel cell simulation and modeling. IOP Conf. Ser. Mater. Sci. Eng. 702, 012017.
Oprych, P.P., Zinko, T., Jaworski, Z., 2017. CFD modelling of hydrogen starvation conditions in a planar Solid Oxide Fuel Cell. Pol. J. Chem. Technol. 19 (2), 16–25.
Pasaogullari, U., Wang, C.Y., 2003. Computational Fluid dynamics modelling of Solid oxide Fuel cells. Electrochem. Soc. Proceedings. 7, 1403–1412.
Radaideh Mohammed, I., Radaideh Majdi, I., 2020. Efficient analysis of parametric sensitivity and uncertainty of fuel cell models with application to SOFC. Int. J. Energy Res. 1–18, 2020.
Singhal, S.C., 2002. Solid oxide fuel cells for stationary, mobile, and military applications. Solid State Ionics 152 –153, 405–410.
Singhal, S.C., Kendall, K., 2003. High Temperature Solid Oxide Fuel Cells: Fundamentals, Design and Applications. Elsevier, Oxford.
Takino, K., et al., 2019. Simulation of SOFC performance using a modified exchange current density for pre-reformed methane-based fuels. Int. J. Hydrogen Energy.
Wu, C., et al., 2019. Global sensitivity analysis of uncertain parameters based on 2D modeling of solid oxide fuel cell. Int. J. Energy Res. 1–19. John Wiley & Sons, Ltd.
Yaws, C.L., 2015. The Yaws Handbook of Physical Properties for Hydrocarbons and Chemicals. Gulf Professional Publishing.
Yonekuraa, T., et al., 2011. Exchange current density of solid oxide fuel cell electrodes. ECS Transactions 35 (1), 1007–1014.
Yuan, J., 2010. Simulation and analysis of multi-scale transport phenomena and catalytic reactions in SOFC anodes. Chem. Prod. Process Model. 5 (1), 15–25.